

¹H NMR-based metabolomic analysis of a human melanoma cell line

Myriam Malet-Martino¹, Thomas Cruz¹, Stéphane Balayssac¹, Jérôme Kluzza², Philippe Marchetti², Véronique Gilard¹

¹Biomedical NMR Group, Laboratoire SPCMIB, UMR CNRS 5068, Université Paul Sabatier, 118 route de Narbonne, 31062 Toulouse Cedex 9, France
²UMR837 Equipe 4 Inserm and Faculté de Médecine, Université de Lille II, 1 Place Verdun, 59045 Lille Cedex, France

Introduction

Melanoma is a malignant tumor of the skin or mucous membranes. Melanoma cells have an abnormal energy metabolism characterized by an increased aerobic glycolysis and reduced mitochondrial energy functions, referred to as the "Warburg effect" [1]. These metabolic disorders facilitate the development of the tumor and the invasion of peripheral tissues. Among proteins which play a role in this abnormal energy metabolism, we are interested in HIF-1 α (Hypoxia-Inducible Factor-1 α). HIF-1 α is known to activate the expression of glycolytic enzymes and glucose transporters and to downregulate mitochondrial activity [2]. The presence of this protein leads to modifications at the level of the glycolysis and the tricarboxylic acid cycle (TCA cycle). Moreover, in hypoxic conditions, tumor cells maintain their proliferation by running the TCA cycle in a "reverse" direction where glutamine contributes to fatty acid synthesis.

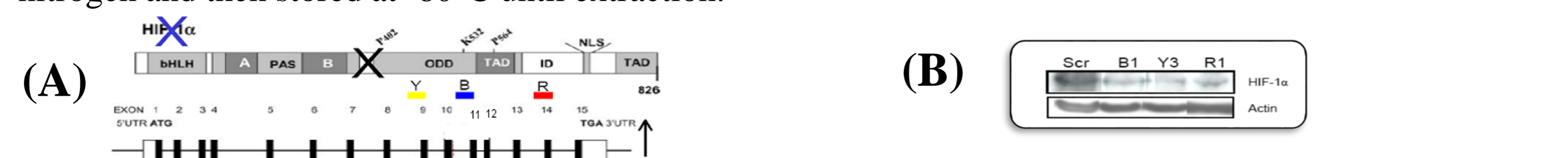
The HBL human melanoma cell line was studied. We compared the ¹H Nuclear Magnetic Resonance (NMR) metabolomes of HBL scrambled cells (WNC) that possess an overexpression of the HIF-1 α protein with those of three HBL knockdown cells in which one of the "programmers" of the metabolism, the transcription factor HIF-1 α , was inhibited (B1, R1 and Y3).



Experimental part

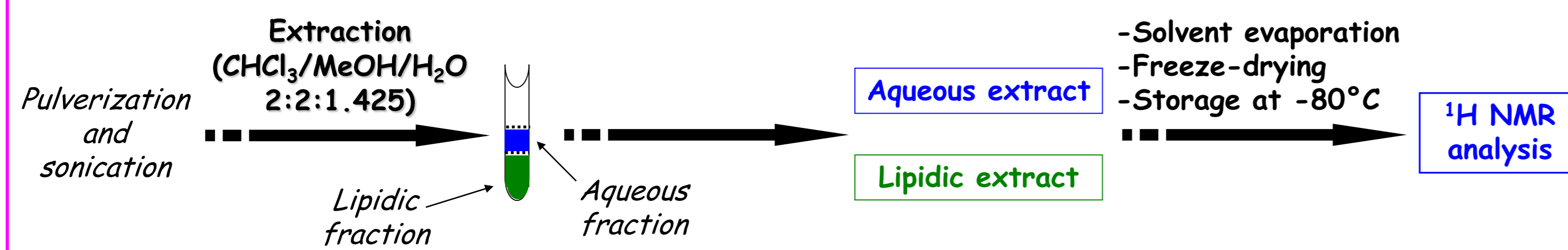
Cell cultures

Cell lines (passage number 10) were cultured at 37°C under 5% CO₂ in RPMI medium supplemented with 10% fetal calf serum, antibiotics, and 1 mM sodium pyruvate. Cells were harvested at 70% confluence. 40 samples (10 for each family) of 10 M cells were prepared. Cells were immediately frozen in liquid nitrogen and then stored at -80°C until extraction.



(A) Three HIF-1 α short hairpin RNA (shRNA) clones were obtained. They target different exons of the HIF-1 α gene: exon 9 for Y3, exon 11 for B1 and exon 14 for R1. (B) HIF-1 α expression by immunoblot analysis.

Cell and tissue extraction



NMR

1D ¹H NMR experiments were recorded at 298K on a Bruker Avance 400 spectrometer equipped with a 5 mm BBI probe. Acquisition parameters for 1D pulse sequence (relaxation delay-pulse-acquisition) were as follows: repetition time of 5.4 s, 32K data points, spectral width of 12 ppm (4800 Hz) and 3072 scans for aqueous extracts, and repetition time of 7.8 s, 64K data points, spectral width of 14 ppm (5600 Hz) and 512 scans for organic extracts. A flip angle of 30° and a relaxation delay of 2.0 s with CW pre-saturation pulse for HOD signal suppression (for aqueous extracts) were used in for both types of extracts.

Statistical analyses

The bin area method based on intelligent bucketing (KnowItAll®, BIORAD) was used for segmenting NMR spectra. After probabilistic quotient normalization, univariate and multivariate analyses as well as statistical correlations based on Pearson correlation coefficients were performed using a toolbox developed in the R environment [3] and SIMCA P+ software (Umetrics®). Each statistical model was validated thanks to the Q² (predictive value of the model) and CV-ANOVA (ANalysis Of VAriance testing of cross-validated predictive residuals) values.

NMR assignments

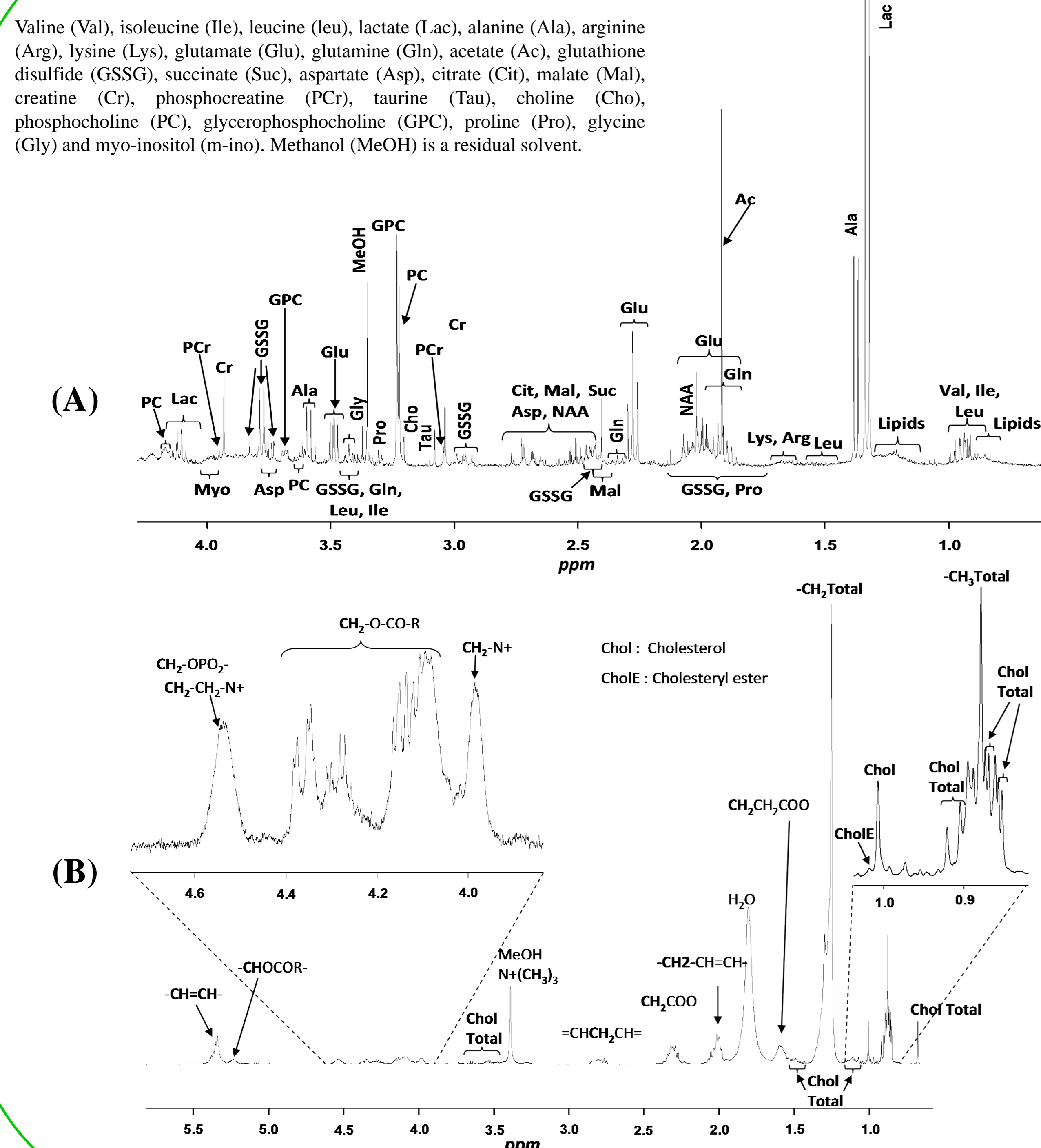


Figure 1. ¹H NMR spectra of typical aqueous (A) and lipidic (B) extracts from B1 cells lines.

Comparison between scrambled cells and knockdown cells

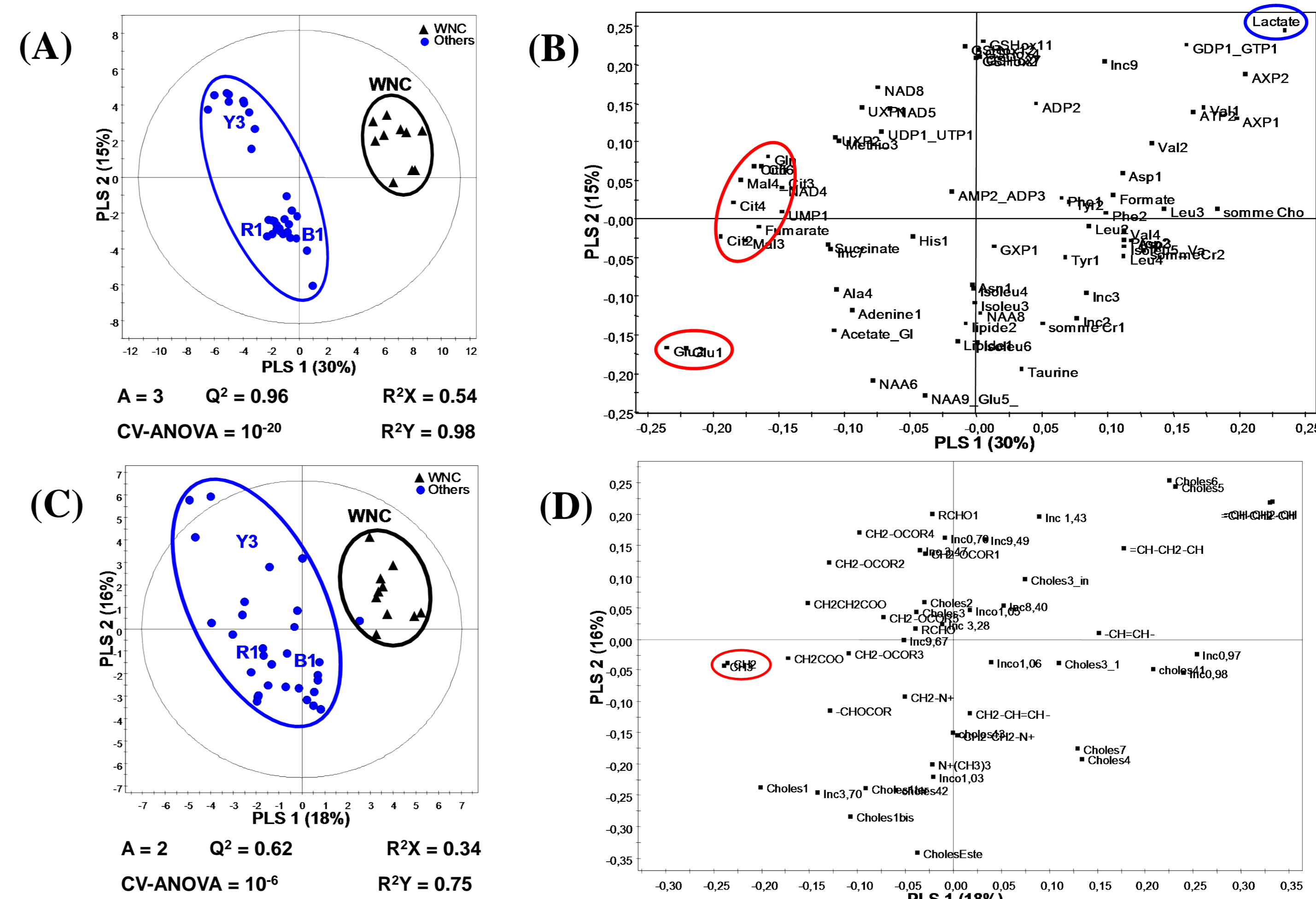


Figure 2. Score plots (A,C) and loading plots (B,D) of the PLS-DA on NMR data of scrambled (WNC) and knockdown (B1, R1 and Y3) HBL cells for aqueous (up) and organic (down) extracts.

The results of the PLS-DA presented in Figure 2 were obtained from ¹H NMR data of 40 samples. A good clustering is observed. Discrimination is based mainly on two metabolites, lactate and glutamate, but also on three TCA-related metabolites (citrate, fumarate, malate) and on glutamine (the precursor of glutamate) for aqueous extracts. In the lipidic fractions, the discrimination is based on fatty acid CH₂ and CH₃ groups.

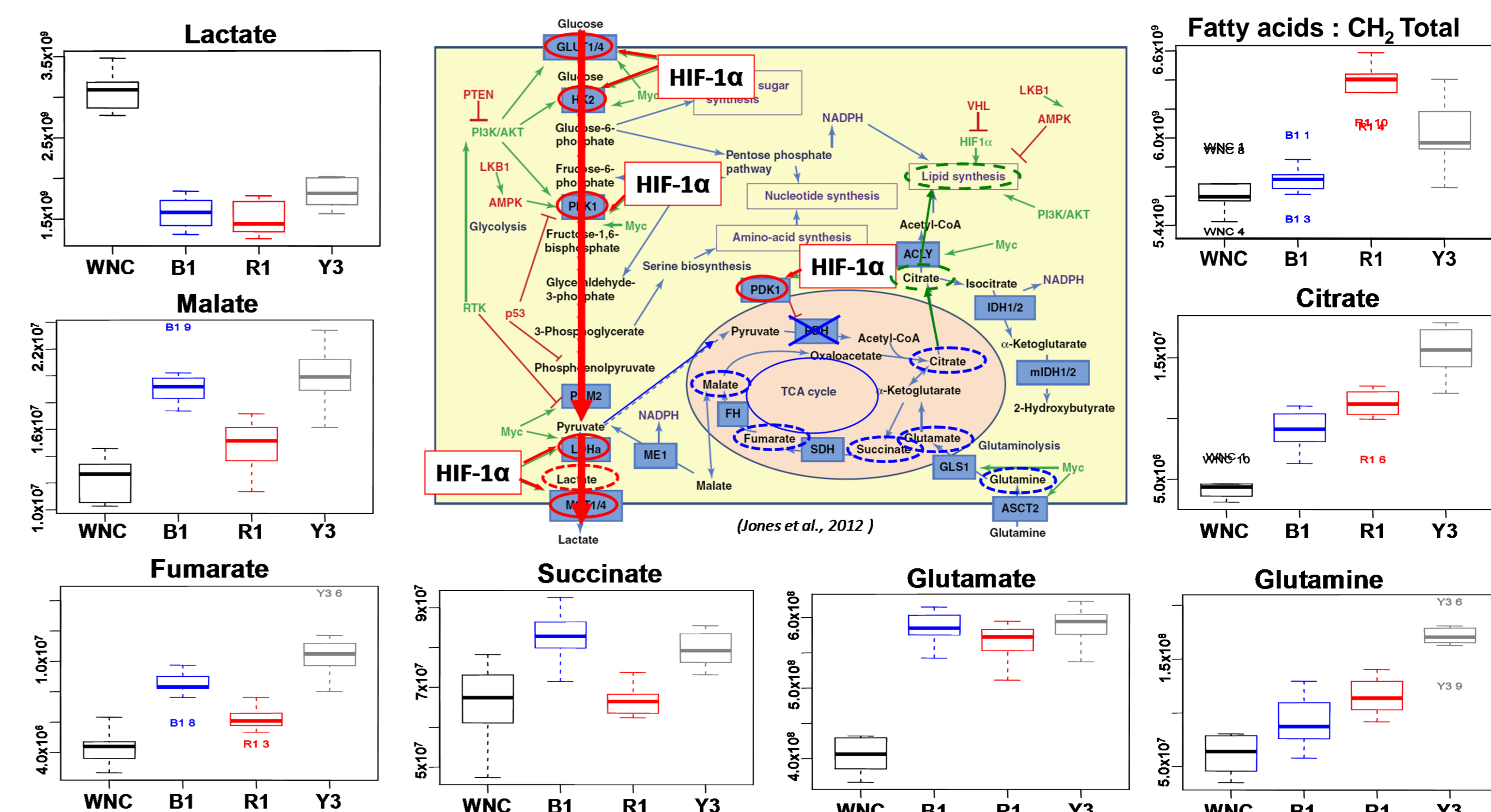


Figure 3. Box plots for lactate, malate, fumarate, succinate, glutamate, glutamine, citrate and fatty acids from NMR data of scrambled (WNC) and knockdown (B1, R1 and Y3) HBL cells.

When HIF-1 α is inhibited, the same behavior at the level of the glycolysis and in the TCA cycle is observed for B1, R1 and Y3 with respect to scrambled cells (WNC). The decreased amount of lactate reflects perturbation of the glycolysis. The increased quantities of the TCA cycle metabolites reveal mitochondrial activation. Moreover, concentrations of glutamine and glutamate, a second way of entry into the TCA cycle, increase as well as that of fatty acids. These observations suggest that the TCA cycle activation could occur in "reverse" direction with glutamine contributing to fatty acid synthesis.

Statistical correlations between aqueous and lipidic extracts

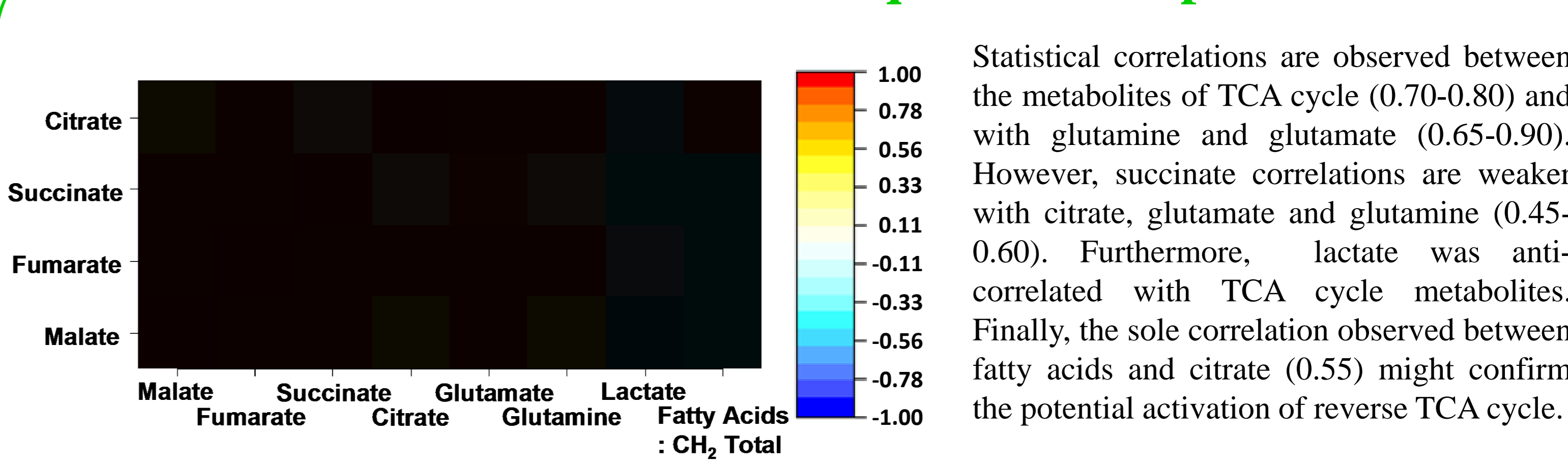


Figure 4. Correlation heatmap for malate, fumarate, succinate, citrate, glutamate, glutamine, lactate, and fatty acids from all NMR data (40 samples).

Conclusion

Our data highlight the crucial role of HIF-1 α in the cell model. The reactivation of the mitochondria leads to increased concentrations of the TCA cycle metabolites (citrate, succinate, fumarate and malate). It also generates perturbations in the glycolysis pathway leading to a decrease in lactate concentration. Moreover, higher concentrations of glutamine, glutamate and fatty acids and statistical correlation between citrate and fatty acids suggest a second way of entry into the TCA cycle with a reverse direction when the expression of HIF-1 α is inhibited.

Ref [1] Hersey P. et al. Clinical Cancer Research 2009; 15: 6490-6494
[2] Kluzza J. et al. Cancer Research 2012; 72: 5035-5047
[3] Balayssac S. et al. Chemometrics and Intelligent Laboratory Systems 2013; 128: 50-59